Crystal structure of the SarR protein from *Staphylococcus aureus*

Yingfang Liu*, Adhar Manna†, Ronggui Li*, Wesley E. Martin*, Robert C. Murphy*, Ambrose L. Cheung†, and Gongyi Zhang*‡

*National Jewish Medical and Research Center and Departments of Immunology and Pharmacology, School of Medicine, University of Colorado Health Science Center, 1400 Jackson Street, Denver, CO 80206; and †Departments of Microbiology and Immunology, Dartmouth Medical School, Hanover, NH 03755

Communicated by John W. Kappler, National Jewish Medical and Research Center, Denver, CO, January 5, 2001 (received for review December 15, 2000)

The expression of virulence determinants in *Staphylococcus aureus* is controlled by global regulatory loci (e.g., *sarA* and *agr*). The *sar* (*Staphylococcus* accessory regulator) locus is composed of three overlapping transcripts (*sarA* P1, P3, and P2, transcripts initiated from the P1, P3, and P2 promoters, respectively), all encoding the 124-aa SarA protein. The level of SarA, the major regulatory protein, is partially controlled by the differential activation of the *sarA* promoters. We previously partially purified a 13.6-kDa protein, designated SarR, that binds to the *sarA* promoter region to down-modulate *sar*A transcription from the P1 promoter and subsequently SarA expression. SarR shares sequence similarity to SarA, and another SarA homolog, SarS. Here we report the 2.3 Å-resolution x-ray crystal structure of the dimeric SarR-MBP (maltose binding protein) fusion protein. The structure reveals that the SarR protein not only has a classic helix–turn–helix module for DNA binding at the major grooves, but also has an additional loop region involved in DNA recognition at the minor grooves. This interaction mode could represent a new functional class of the ''winged helix'' family. The dimeric SarR structure could accommodate an unusually long stretch of ≈27 nucleotides with two or four bending points along the course, which could lead to the bending of DNA by 90° or more, similar to that seen in the catabolite activator protein (CAP)–DNA complex. The structure also demonstrates the molecular basis for the stable dimerization of the SarR monomers and possible motifs for interaction with other proteins.

Staphylococcus aureus is a versatile bacterium capable of causing a wide spectrum of pathology in humans, ranging from superficial abscesses to pneumonia, endocarditis, and sepsis (1). This versatility may be attributable to the impressive array of extracellular and cell-wall-associated virulence determinants coordinately expressed during the process of infection (2). The coordinate expression of many virulence determinants in *S. aureus* has been shown to be regulated by global regulatory elements such as *sarA* (*Staphylococcus* accessory regulator) and *agr* (accessory global regulator) (3, 4). These regulatory elements, in turn, control the transcription of a wide variety of unlinked genes, many of which have been implicated in pathogenesis.

The global regulatory locus *agr* encodes a two-component, quorum sensing system that is involved in the generation of two divergent transcripts, RNAII and RNAIII, from two distinct promoters, P2 and P3, respectively. RNAIII, initiated from the P3 promoter, is the regulatory molecule of the *agr* response, hence responsible for the up-regulation in extracellular protein production and the down-regulation of cell-wall-associated protein synthesis during the postexponential growth phase (5, 6). The RNAII molecule, driven by the P2 promoter, encodes a four-gene operon, *agrBDCA*. Additionally, *agrD*, in conjunction with *agrB*, participates in the generation of an octapeptide with quorum sensing functions (7, 8). This autoinducing peptide can stimulate the transcription of the *agr* regulatory molecule RNAIII, which ultimately interacts with target genes to modulate transcription (6) and possibly translation (9).

In contrast to *agr*, the *sarA* locus activates the synthesis of both extracellular (e.g., α- and β-hemolysins) and cell-wall proteins (e.g., fibronectin binding protein A) in *S. aureus* (3). The *sarA* locus is composed of three overlapping transcripts [*sarA* P1 (0.56 kb), *sarA* P3 (0.8 kb), and *sarA* P2 (1.2 kb) transcripts]. Because of their overlapping nature, each of these transcripts encodes the major 372-bp *sarA* gene, yielding the 14.5-kDa SarA protein (10). DNA footprinting studies revealed that the SarA protein binds to the promoters of several target genes (11) including *agr*, *hla* (α hemolysin gene), *spa* (protein A gene), and *fnbA* (fibronectin binding protein A gene), thus implicating SarA as a regulatory molecule that can modulate target gene transcription via both *agr*-dependent and *agr*-independent pathways (11–13).

The complexity of the *sarA* triple promoter system also hints at the possibility that regulatory proteins may bind to the *sarA* promoter region to modulate *sarA* transcription and, subsequently, SarA expression. Using a DNA-affinity column, we recently identified a 13.6-kDa protein, designated SarR (14), that shares homology with SarA and SarH1 (also called SarS), another SarA homolog (15). SarR binds upstream of the *sarA* P1 and P3 promoter region to modulate SarA expression (16). A mutation in *sarR* decreases transcription from the P1 promoter, the predominant *sarA* promoter, and hence the ensuing SarA expression. To provide a framework for understanding how SarR behaves as a DNA-binding protein, which have dual functions of repressor as well as activator, we solved the crystal structure of SarR.

Materials and Methods

Protein Expression, Purification, and Crystallization. The intact 345-bp *sarR* gene was amplified by PCR using chromosomal DNA from *S. aureus* strain RN6390 as the template and primers containing flanking restriction sites (*Nde*I and *Bam*HI) to facilitate cloning into an expression vector pMAL-c2 (New England Biolabs) modified by truncating 21 residues from the linker region that connects SarR and maltose binding protein (MBP; R.L. and G.Z., unpublished data). The recombinant plasmid containing the *sarR* gene was transformed to *E. coli* BL21(DE3)pLysS. Enhanced expression of SarR-MBP fusion was induced by adding IPTG (isopropyl 1-thio-β-D-galactopyranoside) to a 4-l growing culture (37°C) at an OD_{650} of 0.7. After 4 h of additional growth, cells were harvested, resuspended in buffer (50 mM Tris·HCl, 1 mM EDTA, pH 7.4, 300 mM NaCl, 5% glycerol, and 1 mM DTT) and subjected to cell lysis through

Abbreviation: MPB, maltose binding protein; *sar*, *Staphylococcus* accessory regulator; *agr*, accessory global regulator; CAP, catabolite activator protein.

Data deposition: The atomic coordinates have been deposited in the Protein Data Bank, www.rcsb.org (PDB ID code 1HSJ).

‡To whom reprint requests should be addressed at: 1400 Jackson Street, 501b, Denver, CO 80206. E-mail: zhangg@njc.org.

The publication costs of this article were defrayed in part by page charge payment. This article must therefore be hereby marked "*advertisement*" in accordance with 18 U.S.C. §1734 solely to indicate this fact.

Table 1. Summary of crystallographic analysis

Crystal*	Resolution, Å	R_{merge}†, %	Reflections measured/unique	Completeness, %	Solutions¶	CO¶	R¶
			Diffraction data and MR statistics				
Native I	2.8	4.3	62,396/20,967	78.0	2	47.2	46.6
Native II	2.3	2.7	77,545/37,403	96.5			

	Refinement (Native II)								
Resolution, Å	20–4.58	3.65	3.19	2.90	2.69	2.53	2.40	2.30	Total
No. reflections	5696	5656	5512	5198	4788	4180	3454	2702	37,186
R-factor‡	15.27	20.16	29.30	33.14	36.95	38.04	38.86	41.56	23.24
Free R-factor§	21.94	24.45	32.45	38.65	39.36	38.79	35.91	38.02	28.22

rms deviations; Bonds, 0.009 Å; Angles, 1.4°

*Crystal spacegroup P1; a = 64.7 Å, b = 70.6 Å, c = 75.5 Å, α = 65.7°, β = 67.2°, γ = 69.6°, two SarR-MBP monomers/unit cell.
†$R_{merge} = 100 \times \Sigma_j|I_j - \langle I\rangle|/\Sigma_j I_j$ with Bijvoet pairs treated as equivalent.
‡R-factor $= \Sigma|F_{obs} - F_{calc}|/\Sigma F_{obs}$ for all amplitudes with $F/\sigma(F) \geq 2$ measured in the indicated resolution bin.
§Free R-factor was calculated with 5% of the data in each bin.
¶Molecular replacement solutions, CO, (correlation coefficients); and R, are defined in AMORE (19).

a continuous-flow French press. After a 20,000 × g spin, the soluble fraction was loaded onto an amylose resin affinity column (10 ml) and the SarR-MBP fusion protein was eluted with 10 mM maltose. The protein was loaded onto a MonoQ (Amersham Pharmacia) ion-exchange column. After elution with a NaCl gradient (0.1 to 0.5 M), the fraction containing the protein was found to be homogeneous as determined by a Coomassie-stained SDS-polyacrylamide gel. The concentration of the purified protein was determined with the Bio-Rad Protein Assay solution, using BSA as the standard. The SarR-MBP fusion protein (15 mg/ml) was crystallized by vapor diffusion against a solution of 5 mM β-mercaptoethanol, 100 mM Na acetate, 100 mM NaCl, pH 4.6, and 18–22% PEG monomethyl ether 2000. For cryo-crystallography, crystals were soaked in steps of increasing glycerol concentration (5% each step every 30 min) and finally into 20% glycerol before flash-freezing.

Structure Determination and Refinement. Data were collected in the laboratory on a Rigaku R-axis IV system and beamline 5.0.2 at the Advanced Light Source (ALS) at Berkeley. Data processing was performed with DENZO and SCALEPACK (17). The initial phases were obtained by a molecular replacement solution using the available MBP structure (18) and the program AMORE (19). Fo-Fc and 2Fo-Fc electron density maps were calculated by CNS (20). Map interpretation and model building were done by using the program O (21) and aided by the secondary prediction results (22). The map was improved by cycles of refinement using CNS with Non-Crystallographic Symmetry (NCS) constraints. A final refinement was performed with relaxed NCS restraints

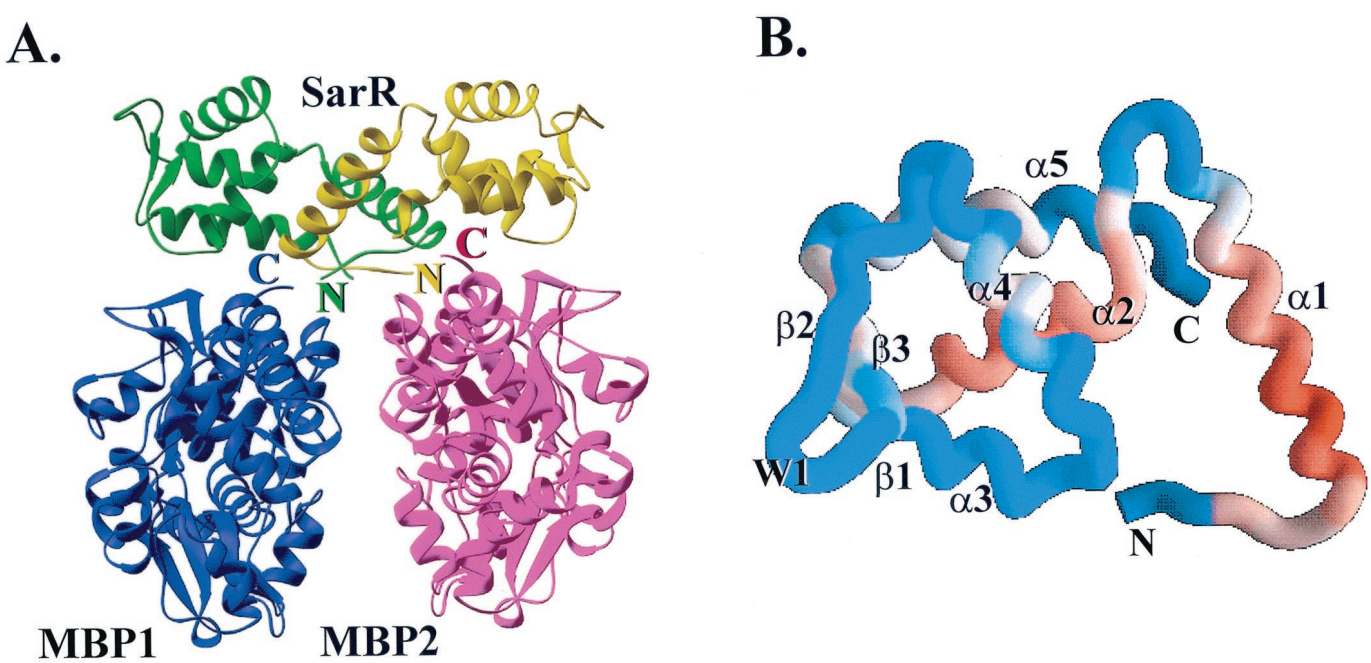

Fig. 1. (*A*) A ribbon (27) diagram of the three-dimensional structure of the SarR-MBP fusion protein. The SarR dimer is at the top colored green and yellow for each monomer, respectively, and the two MBP molecules are at the bottom colored blue and pink, respectively. (*B*) A worm diagram of the three-dimensional structure of the SarR monomer. Starting from the N terminus, α1 (6–24) → α2 (32–44) → β1 (47–50) → α3 (residue 51–58) → α4 (63–74) → β2 (79–83) → β3 (90–96) → α5 (97–113). α2, β1, α3, α4, β2, and β3 are defined as a ''winged helix motif.'' The worm is colored according to the B factor of the side chain: red (low B, 25), white (middle B, 45), and blue (high B, 80).

(Table 1). The final model contains residues 1–115 for molecule 1 of SarR, residues 1–115 for molecule 2 of SarR (Fig. 1*B*), residues 1–372 for both MBP molecules (Fig. 1*A*), two maltose molecules, and 190 water molecules. Stereochemical values are all within or better than the expected ranges for a 2.3-Å structure, as determined by using PROCHECK (23).

Results and Discussion

Overall Structure. The structure of SarR-MBP fusion protein shows that the SarR dimer is located at the top of the two individual MBP molecules, connected by two loops (with residues both from SarR and modified MPB) between SarR and MBP. The positions of the MBP molecules suggest that they did not influence the structure of SarR dimer (Fig. 1*A*). The overall structure of the SarR monomer consists of five α helices, three short β strands, and several loops (Fig. 1*B*). The α1 helix extends out from the remaining molecule, forming an "L"-like structure with a stretch formed from the N-terminal residues of the protein. The α2 helix follows a 7-residue loop from α1, and is almost perpendicular to α1 (85°). The three β strands, β1, β2, and β3, form an antiparallel bundle, which is slightly twisted. α5 follows immediately after β3. Between β1 and β2 is a long flexible region (residues 51–79), which had poor electron density in the initial 2Fo-Fc and Fo-Fc maps, containing two helices, α3 (residue 51–56) and α4 (residue 63–75), respectively, and a short turn (residue 56–58); these three elements build up a typical helix–turn–helix structural module existing in DNA binding proteins. Homology alignment (DALI; ref. 24) of the SarR structure with all available structures shows that the SarR monomer is homologous to winged helix proteins (25), such as transcription regulatory protein mota fragment (PDB ID code 1bja) with a *Z* score of 8.0 and transcriptional repressor smtb activation domain (PDB ID code 1smt) with a *Z* score of 7.2. Compared with winged helix proteins, the "W2" is replaced by a helix (α5) and the "W1" extends much further in the SarR monomer (Fig. 1*B*). Therefore, we postulate that SarR and its family of proteins likely are new members of the classic winged helix protein family.

Two L-like structures of α1 and the stretch of the N-termini come together, forming a dimer that has an elongated, slightly bent structure with overall dimensions of 71 Å × 37 Å × 34 Å (Fig. 2 *A*, *B*, and *C*). The monomers are related to each other by a noncrystallographic local 2-fold axis. On the concave side and middle of the SarR dimer, there is a canyon-like structure with a length of ≈35 Å, a width of ≈25 Å, and a depth of ≈10 Å (Fig. 2 *A* and *B*). The canyon is formed by a part of α1, the loop that connects α1 and α2 and a part of α2 as its bed, and with α4 from both monomers acting as the two banks (Fig. 2 *A* and *B*). On the convex side, all four termini (C- and N-termini of both molecules) form a flat platform with the N terminus of one monomer adjacent to the C terminus of the other (Fig. 2*C*). This feature may possibly explain how SarS, a 250-residue protein homologous to SarA (26), may function as a heterodimer-like monomer because it contains two sections, each highly similar to the SarR module and 125 residues long (26). The entire dimer can be described as three individual subdomain structures (Fig. 2*A*). Three β strands plus α3 and α4 from each molecule form subdomains 1 and 2, respectively. Those two subdomains were poorly defined in the initial electron density map, which also was reflected by their high temperature factors compared with the rest in the final model (Fig. 1*B*), and thus can be expected to have high mobility in the molecule in solution. Subdomain 3, consisting of the major α helices α1, α2, and α5 from both monomers, is relatively rigid because of the restraints of hydrophobic interactions. These helices in subdomain 3 are arranged in such a manner that the entire subdomain looks like a twisted letter Z with the relatively flexible subdomain 1 and subdomain 2 covering its ends. The Z-shaped scaffold, a unique structural feature for SarA family, could also represent a new functional protein fold (Fig. 2 *A* and *C*).

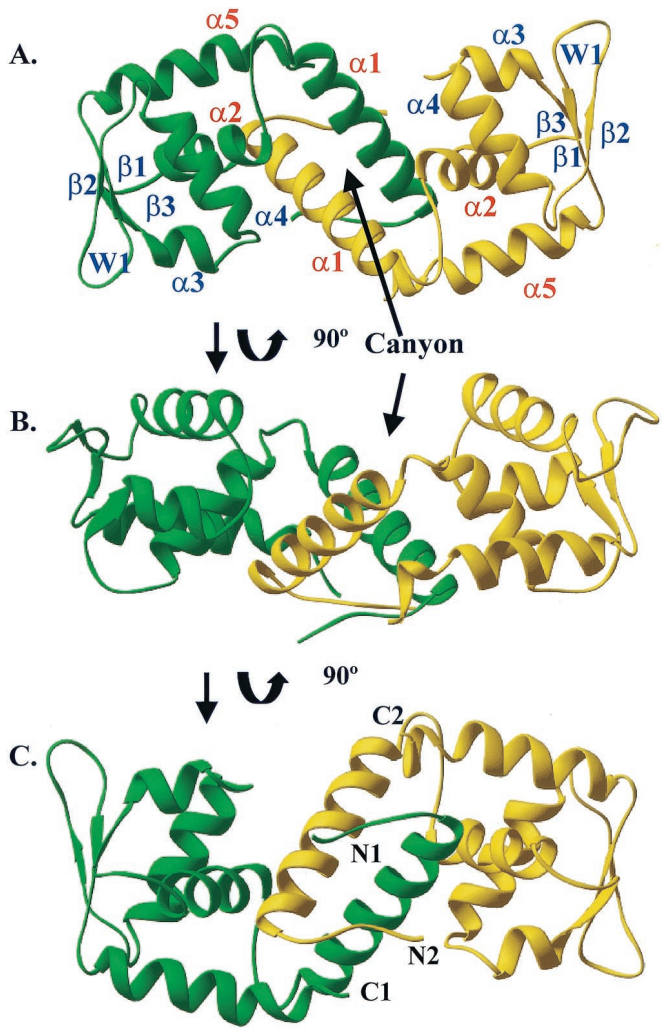

Fig. 2. Structure of the SarR dimer. One SarR monomer is colored green, the other is yellow. (*A*) View of concave side along the dimer 2-fold axis of the SarR dimer, subdomain 1 contains β1, α3, α4, β2, and β3 (labeled blue) from one monomer, subdomain 2 contains β1, α3, α4, β2, and β3 (also labeled blue) from the other, and subdomain 3 contains α1, α2, and α5 (labeled red) from both monomers. (*B*) View perpendicular to the dimer 2-fold. (*C*) View of the convex side of the SarR dimer; N1 and C1 are the N terminus and C terminus of molecule 1; N2 and C2 are the termini of molecule 2.

Dimerization Interfaces. Several lines of evidence suggest that, with the exception of SarS, the active form of the SarA family of proteins may be a homodimer. First, there is strong evidence showing that SarA exists as a homodimer *in vitro* as well as *in vivo* (15). Second, on mixing partially unfolded (4 M urea) full-length SarR protein and SarR-MBP fusion, a heterodimer product containing one copy each of SarR and SarR-MBP fusion could be separated by gel-filtration chromatography (data not shown). Third, we used crystals of SarR-MBP fusion protein to solve the SarR structure (see *Materials and Methods*). The SarR exists as dimer even in the MBP fusion form and we postulate that the dimerization form may be the active form existing *in vivo*. Fourth, based on the homodimer SarR structure, the interactions between the two monomers are quite extensive, with most residues involved in hydrophobic interactions (Figs. 1*A* and 3). Residues Leu-10, Ile-7, and Ile-4 from one monomer and

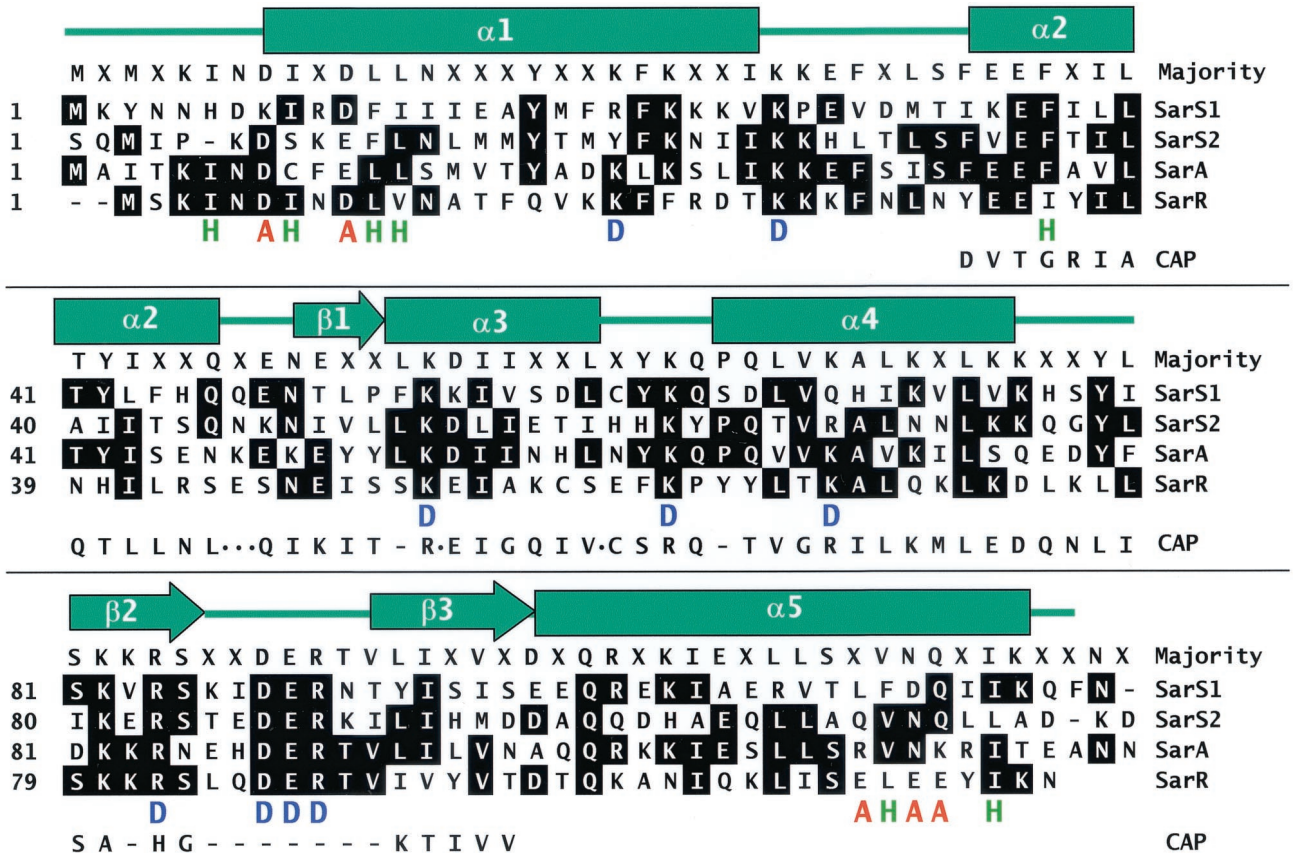

Fig. 3. A sequence alignment of SarA homologs from *S. aureus*. The sequences are presented in one-letter amino acid code. Numbers at the beginning of each line indicate amino acid positions relative to the start of each protein sequence. Helices are indicated by rectangles, β-sheets are indicated by arrows, and loops are indicated by a line. ''H'' marked in green represents a residue that takes part in dimerization. ''A'' marked in red represents a residue that may compose of the activation motifs. ''D'' marked in blue represents a residue that may be involved in the interaction of SarR with DNA. The sequence of DNA binding motif from CAP is also aligned to the SarA proteins. A dot represents a residue(s) omitted and a dash represents a residue(s) missed in CAP. SarS2 starts at 1 (actual position on SarS is 126).

residues Phe-20, Ile-35, Leu-109, and Ile-113 from the other monomer form two hydrophobic cores. The dimer interface buries ≈1,500 Å^2 of solvent-accessible surface area (1.4-Å probe; ref. 28) per monomer. Considering this hydrophobic feature of SarR dimerization, we believe that the dimer of SarR in the fusion protein is also the functional dimer *in vivo*. Furthermore, the L-like structure of α1 and the stretch of the N terminus of SarR physically block the dissociation of one monomer from its partner. This blockage explains why an extremely harsh condition (4 M urea) is required to disrupt the dimerization of individual monomers. Fifth, deletion analysis showed that mutated SarA, with a 15-residue truncation at its N terminus, exists as monomers *in vitro* (in solution or crystal packing forms; data not shown). Finally, as predicted from the sequence alignment of SarA, SarR, and SarS, most residues that are involved in the dimerization process are highly conserved (Fig. 3).

DNA Binding and Bending. As reported earlier, SarA and SarR proteins contain a high percentage of the residue Lys (29). Remarkably, most of the Lys residues are highly conserved between these two proteins (Fig. 3). It was predicted that most of these Lys residues are involved in DNA binding (29). Although the Lys residues are distributed throughout the entire primary sequence, in the 3D structure most Lys residues and some Arg residues are located primarily on one surface of the SarR dimer (the concave side). The electrostatic potential on this surface of the SarR dimer, calculated by the GRASP program (28), revealed a positively charged track on this side (Fig. 4*A*). Additionally, the two winged helix motifs (subdomain 1 plus α2 from one monomer and subdomain 2 plus α2 from another monomer) are located on this side. We conclude that this side is the most likely site for DNA binding.

Using the program DALI to search for proteins with a structure similar to SarR, we examined manually every structure with a *Z* score higher than 4. We found that the spatial arrangement of the two SarR helix–turn–helix modules is quite similar to those described for catabolite activator protein (CAP; ref. 30; PDB ID code 1cgp with *Z* score of 4.7). Superposing the SarR winged helix motifs 1 and 2 with the corresponding domains from CAP dimer, the root mean square deviation (rmsd) of the α-carbon backbone is 1.8 Å for motif 1, and 2.1 Å for motif 2 (Fig. 5*A*). Interestingly, some of the residues involved in DNA binding and bending in the CAP dimer, which interacts with the major grooves, are conserved in the SarR dimer and in other members of the SarA family (Fig. 3). For example, SarR-charged residues that are predicted to interact with phosphate groups on the DNA backbone are possibly Lys-52, Lys-56, Lys-71, and Arg-82. Lys-52 and Arg-82 are absolutely conserved in the SarR and SarA family of proteins. Charged residues predicted to contact DNA bases are Lys-61 and Lys-67. Lys-61 is also absolutely conserved. Therefore, we predict that the SarR dimer and other SarA family members have protein–DNA interaction similar to the CAP dimer.

The interaction could cause the DNA to bend at two points by ≈90° (30). The longest direct distance for the CAP and SarR dimer surface is ≈71Å (Fig. 4), which can hold a stretch of bent

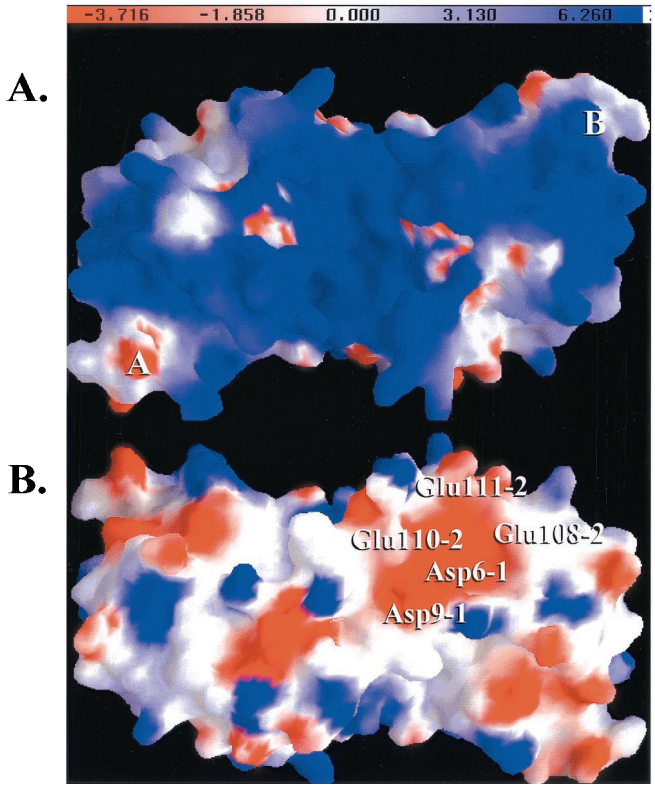

Fig. 4. The electrostatic potential surface of the SarR dimer calculated by GRASP (28), with charge +1 for Lys and Arg, charge −1 for Glu and Asp, and charge zero for all other residues. The color bar from red to blue represents potential from negative to positive defined as in GRASP. The blue represents positive charged potential and red represents negative charged potential. (*A*) The potential surface of the concave side of SarR dimer (similar orientation as Fig. 2*A*), the direct line distance of AB is ≈65 Å. (*B*) The potential surface of the convex side of the SarR dimer (similar orientation as Fig. 2*C*), two aspartic acid residues are from one molecule, three glutamic acid residues from the other.

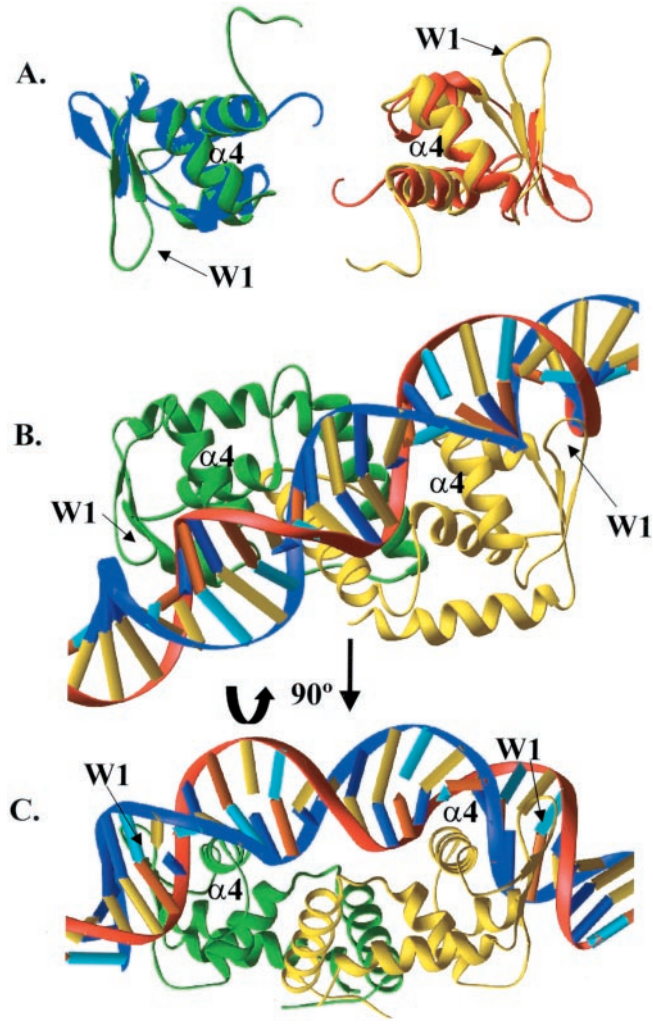

Fig. 5. (*A*) Superposition of two ''winged helix motifs'' (subdomain 1 plus α2 from one monomer and subdomain 2 plus α2 from another monomer) of SarR dimer with the DNA binding domains of CAP (PDB ID code 1cgp), subdomains from SarR marked green and yellow respectively, subdomains from CAP marked blue and red. α4 and W1 interact with DNA at major grooves and minor grooves, respectively. (*B*) The DNA binding model of SarR and DNA (similar orientation as in Figs. 2*A* and 5*A*). The SarR dimer is superposed to that of CAP. The DNA structure is from the CAP–DNA complex structure (PDB ID code 1cgp). The wing region (W1) conformation is slightly adjusted to fit in the minor groove. (*C*) A 90° orientation from the view of Fig. 5*B*.

DNA with ≈27 base pair nucleotides that has a length of ≈92 Å for a normal B form (30). This result is consistent with the experimental DNA footprinting data, showing that ≈29 nucleotides from the *sarA* promoter region were involved in binding to SarR (31). This predicted bending of the DNA when SarR binds to DNA may reflect a regulatory mechanism for the SarA family of proteins in controlling target gene transcription.

We superimposed the SarR dimer on the CAP–DNA complex to construct a model for a SarR–DNA complex (Fig. 5 *B* and *C*). From this model, we can predict that, in addition to interactions of the α4 helix with the DNA major groove, SarR may make contacts with the DNA minor groove. The loop region between β2 and β3 and part of the two β strands (W1, a β-hairpin) are predicted to be quite flexible in the free SarR structure. Only slight adjustments of their conformations are required to position them to interact intensively with the minor groove of the DNA. Several residues that could be involved in the interactions are highly conserved residues (Asp-86, Glu-87, and Arg-88), with perhaps the side chain of Arg-88 interacting with the DNA phosphate backbone and the side chains of Asp-86 and Glu-87 interacting with bases (Fig. 5 *B* and *C*). There is no data so far to show whether additional bending could be induced by this interaction. This loop is too short in CAP and other winged helix proteins to have this minor groove binding function (25). One new member of one of the classes of winged helix proteins (RFX) does make DNA minor groove contacts, but in this case, the wing contacts the major groove and the helix contacts the minor groove (32). Therefore, the predicted SarR type of wing-minor groove interaction may be a unique feature of the SarA family of proteins, thus establishing them as a third class of the winged helix family (25, 32). The structure of DNA complexed with a member of SarA family is needed to test this prediction.

The two subdomains that are involved in DNA binding and bending in CAP have different conformations in the absence of DNA, but are identical in the complex structure (25). The corresponding subdomains (1 and 2) in SarR are almost identical in the free protein, but most of the side chains are poorly defined. We believe that these two subdomains have high mobility in the absence of DNA, as has been described for the CAP protein. The mobility can be indicated by their high temperature factors (Fig. 1*B*).

Possible Regulation Mechanism. One class of transcription-activating proteins bears two structural motifs, namely DNA binding and activation domains (33). The SarR protein was initially defined as a transcriptional repressor protein that binds

the *sarA* promoter region (29), thus leading to reduced transcription from the *sar* P1 promoter. Because the *sarA* P1 promoter is the predominant promoter in the *sarA* regulatory system, we predicted and recently confirmed that the expression of SarA was increased in a *sarR* mutant (29). Transcriptional fusion studies also indicated that the *sarA* locus may be autoregulatory (31), possibly mediated by the binding of SarA to its own promoter. It was postulated that an activation motif might be present on the SarA protein but not on the SarR protein, and that SarR may repress by a simple competitive displacement mechanism. Indeed, we have found that the binding affinity of SarR to a *sarA* promoter fragment is higher than its SarA counterpart (16). A second possibility is that SarA and SarR may form a heterodimer to interfere with the function of the SarA homodimer. Because of the conservation of residues involved in the dimerization, this could happen *in vivo*, although we have so far failed to generate a heterodimer of SarA and SarR when using His-tag proteins *in vitro*. Nevertheless, attempts to yield heterodimers with native SarA and SarR proteins without any His-tags are in progress. Finally, SarR may function in a manner similar to the bacteriophage lambda repressor (which also has a helix–turn–helix DNA binding motif). In this case, a slight difference in DNA binding site (one base pair shift) could turn an activator into a repressor by affecting RNA polymerase binding (34).

The structure of the SarR protein, combined with the sequence alignment of additional SarA family members (Fig. 3), suggests that the regulatory mechanism may be much more complicated. Although there is no isolated activation domain in the SarR dimeric structure compared with the CAP, a calculation of the surface electronic potential revealed two negatively charged patches on the convex side of the SarR dimer (Fig. 4*B*). These patches include residues Asp-6 and Asp-9 from molecule 1 and Glu-108, Glu-110, and Glu-111 from molecule 2. Many transcription regulators work by binding DNA and then interacting with a component of the RNA polymerase machinery (33). For example, CAP regulates downstream protein expression mostly through its interactions with the C-terminal domains of the α subunit of RNA polymerase (35). It is tempting to speculate that these acidic patches on the surface of SarR may represent activation motifs that allow SarR to regulate gene expression in a similar way as SarA. Because Glu-108, Glu-110, and Glu-111 are not conserved among the SarA family (Fig. 3), this activity may have different specificities among the family members. In this regard, we have experimental evidence to suggest that SarR, besides interacting with the *sarA* promoter acting as a repressor, also directly binds to the *hla* promoter (e.g., α hemolysin gene) as an activator, thus bypassing the effect of SarA in controlling target gene expression (data not shown).

We thank John Kappler for discussions and advice; Howard Hughes Medical Institute, Zuckerman/Canyon Ranch, and Alan Lapore for support of our x-ray and computing facility; Keith Henderson for assistance at 5.0.2 of the Advanced Light Source (ALS) at Berkeley; Philippa C. Marrack, James D. Crapo, and other members at National Jewish for their kind support; and Elizabeth A. Campbell and Seth A. Darst for initial crystallization experiments with SarR protein. G.Z. is supported by a start-up fund from National Jewish Medical and Research center. A.L.C. is supported by a grant from the National Institutes of Health.

1. Boyce, J. M. (1997) in *The Staphylococci in Human Disease*, ed. Crossley, K. B. & Archer, G. L. (Churchill Livingstone, New York), pp. 309–329.
2. Projan, S. J. & Novick, R. P. (1997) in *The Staphylococci in Human Disease*, ed. Crossley, K. B. & Archer, G. L. (Churchill Livingstone, New York), pp. 55–81.
3. Cheung, A. L., Koomey, J. M., Butler, C. A., Projan, S. J. & Fischetti, V. A. (1992) *Proc. Natl. Acad. Sci. USA* **89,** 6462–6466.
4. Kornblum, J., Kreiswirth, B., Projan, S. J., Ross, H. & Novick, R. P. (1990) in *Molecular Biology of the Staphylococci*, ed. Novick, R. P. (VCH, New York), pp. 373–402.
5. Janzon, L. & Arvidson, S. (1990) *EMBO J.* **9,** 1391–1399.
6. Novick, R. P., Ross, H. F., Projan, S. J., Kornblum, J., Kreiswirth, B. & Moghazeh, S. (1993) *EMBO J.* **12,** 3967–3977.
7. Ji, G., Beavis, R. & Novick, R. P. (1997) *Science* **276,** 2027–2030.
8. Mayville, P., Ji, G., Beavis, R., Yang, H., Goger, M., Novick, R. P. & Muir, T. W. (1999) *Proc. Natl. Acad. Sci. USA* **96,** 1218–1223.
9. Morfeldt, E., Taylor, D., von Gabain, A. & Arvidson, S. (1995) *EMBO J.* **14,** 4569–4577.
10. Bayer, M. G., Heinrichs, J. H. & Cheung, A. L. (1996) *J. Bacteriol.* **178,** 4563–4570.
11. Chien, C.-T., Manna, A. C., Projan, S. J. & Cheung, A. L. (1999) *J. Biol. Chem.* **274,** 37169–37176.
12. Chan, P. F. & Foster, S. J. (1998) *J. Bacteriol.* **180,** 6232–6241.
13. Chien, Y. T., Manna, A. C. & Cheung, A. L. (1998) *Mol. Microbiol.* **31,** 991–1001.
14. Manna, A. C., Bayer, M. G. & Cheung, A. L. (1998) *J. Bacteriol.* **180,** 3828–3836.
15. Tegmark, K., Karlsso, A. & Arvidson, S. (2000) *Mol. Microbiol.* **37,** 398–409.
16. Manna, A. C. & Cheung, A. L. (2001) *Infect. Immun.* **69,** 885–896.
17. Otwinowski, Z. & Minor, W. (1997 *Methods Enzymol.* **276,** 307–326.
18. Quiocho, F. A., Spurlino, J. C. & Rodseth, L. E. (1997) *Structure* **5,** 997–1015.
19. Navaza, J. (1994) *Acta Crystallogr.* **A50,** 157–163.
20. Brunger, A. T., Adams, P. D., Clore, G. M., Delano, W. L., Gros, P., Grosse-Kunstleve, R. W., Jiang, J.-S., Kuszewsk, J., Nilges, N. & Pannu, N. S. (1998) *Acta Crystallogr.* **D54,** 905–921.
21. Jones, T. A., Zou, J.-Y., Cowan, S. & Kjeldgaard, M. (1991) *Acta Crystallogr.* **A47,** 110–119.
22. Rost, B., Sander, C. & Schneider, R. (1994) *Comput. Appl. Biosci.* **10,** 53–60.
23. Laskowski, R. A., MacArthur, M. W., Moss, D. S. & Thornton, J. M. (1993) *J. Appl. Crystallogr.* **26,** 283–291.
24. Holm, L. & Sander, C. (1993) *J. Mol. Biol.* **233,** 123–138.
25. Gajiwala, K. S. & Burley, S. K. (2000) *Curr. Opin. Struct. Biol.* **10,** 110–116.
26. Cheung, A. L., Schmidt, K., Bateman, B. & Manna, A. C. (2001) *Infect. Immun.* **69,** 2448–2455.
27. Carson, M. (1991) *J. Appl. Crystallogr.* **24,** 958–961.
28. Nicholls, A., Sharp, K. A. & Honig, B. (1991) *Proteins Struct. Funct. Genet.* **11,** 281.
29. Manna, A. C., Bayer, M. G. & Cheung, A. L. (1998) *J. Bacteriol.* **180,** 3828–3836.
30. Schultz, S. C., Shields, G. C. & Steitz, T. A. (1991) *Science* **253,** 1001–1007.
31. Chien, Y. & Cheung, A. L. (1998) *J. Biol. Chem.* **237,** 2645–2652.
32. Gajiwala, K. S., Chen, H., Cornille, F., Roques, B. P., Reith, W., Mach, B. & Burley, S. K. (2000) *Nature (London)* **403,** 916–921.
33. Ptashne, M. & Gann, A. (1997) *Nature (London)* **386,** 569–577.
34. Bushman, F. D. (1992) *Curr. Biol.* **2,** 673–675.
35. Ishihama, A. (1993) *J. Bacteriol.* **175,** 2483.